A Visual Inspection System for Monitoring Weld Quality in LNGC Ship Construction

Hyunki Lee*, Simkeun Yuk*, Min Young Kim*, Youngjun Park**, Jonghyung Kim***,and Hyungsuck Cho*

* Department of Mechanical Engineering, KAIST, Daejeon, Korea
(Tel : +82-042-869-3253; E-mail: hklee@lca.kaist.ac.kr)
**Department of Mechatronics Research, Samsung Heavy Industries Co. Ltd.
***School of Mechnical Design and Automation Engineering, Seoul National University of Technology, Seoul, Korea
(Tel : +81-02-970-6357; E-mail: johnkim@snut.ac.kr)

Abstract: In this paper, a visual welding inspection system for LNGC ship construction process is developed, which is mounted on a wall-climbing robot. For this purpose, we designed the inspection hardware system composed of two cameras and specially designed flexible illumination system. Two cameras with different fields of view are adopted for observing various kinds of defects. Using this inspection system, we can detect and classify four important welding defects ; 1) bead shape abnormality, 2) bead pitch abnormality, 3) arc strike, and 4) scratch, which crucially affect the LNGC tank capacity. Since each of them has its own characteristics on its shape and its image intensity, we can use visual sensors to inspect welded regions effectively. The effectiveness of the proposed system and the inspection algorithm is verified through a series of experiments. As experimental results, the accuracy to detect defects successfully is over 90% and the task time for inspection is within 8 seconds.

Keywords: defect inspection, vision sensor, correlation, illumination system

1. INTRODUCTION

The LNGC(Liquid Natural Gas Container) ship is designed to convey the Liquid Natural Gas between countries with three or four tanks for storing the LNG. The inside walls of each tank consist of a large number of thin stainless plate as shown in Fig. 1, and each thin plate is attached on another using TIG welding technique for making a big tank with cubic shape. The total length of welding line on one LNGC tank is about several kilometers. It indicates that the possibility of welding mistakes is strong. Therefore, for welding parts inspection process has become more and more important thing for the LNGC ship building process. However until now the inspection process only depends on very well trained inspector, and few automated systems are applied to it. Due to these reasons the low efficiency on manual inspection process deteriorates the productivity.

Fig. 1 The LNGC tank which consists of many plates

In LNGC tank construction process, there are many kinds of defects on the welded regions of thin stainless plate. Representative defects are as follows. 1) The bead shape abnormality at the bead region, caused by improper welding operation of human workers and defect of welding rod. 2) The bead pitch abnormality at the bead, caused by the same reason as the bead shape abnormality. 3) The arc strike on the surface near the bead, caused by the heat of a fragment of the welding arc. 4) The scratch on the surface near the bead, caused by careless treatment of the stainless plate. These four defects have very critical characteristics which directly affect the tank capacity, and often become a source of explosion. Therefore, the detection of these defects is indispensable to keep satisfactory weld quality.

Table 1 Defects at the LNGC ship tank

	Appeared location	**A Cause**
Bead shape abnormality	Bead area	improper welding operation of human workers and defect of welding rod
Bead Pitch abnormality		
Arc strike	Surface near the bead area	Hot arc spot
Scratch		careless treatment of the stainless plate

Until now, many studies for welding part inspection have been performed. For these purpose, many kinds of methods such as using a ultra sonic sensor[3][2], x-ray sensor[1], and vision sensor[4][6] has been developed to detect the defects. Among them, methods using special source such as x-ray source and ultra sonic sensor have shortcomings which need more complicated equipment. Based on the fact that common welding defects have distinct features and intensity characteristics, many studies have applied the vision sensor[4][6]. In our study, above-mentioned defects have obvious features and intensity characteristics, so we used the vision system for inspection. In addition, since each defect has their own feature characteristics and is easily discriminated from the other, we don't use the specially designed pattern classifier such as SOM[5], but use a classification method based on shape geometry.

The contents of paper is greatly divided two parts as shown in Fig. 2. The first part is related to design and make a hardware system, which is referred in section 2. The second part is on the algorithm to detect the defects, which is described at section 3. At section 4, the experimental results are presented.

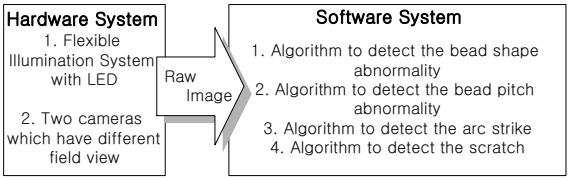

Fig. 2 Schematic of this study

2. INSPECTION HARDWARE SYSTEMS

The inspection system can work with a movable wall-climbing robot as shown in Fig. 3. The robot climbs vertical walls of the tank for inspection of weld quality. Since the working environment is very harsh, specially designed inspection system is needed. Through many experiments, we propose an inspection system which is composed of a flexible illumination system and two cameras which have different fields of view.

Fig 3. Movable wall-climbing robot

2.1 LED Illumination system

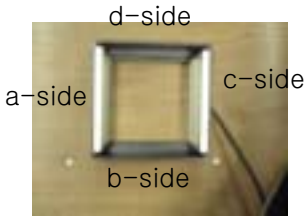

(a) Picture of the square LED illumination

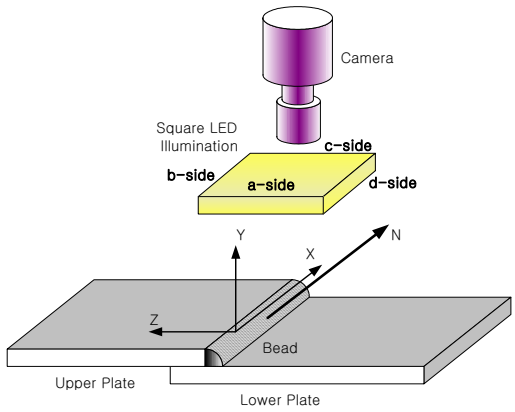

(b) The schematic of illumination system

Fig. 4 The square LED Illumination system

Originally a metal surface has a specular reflection, so that the intensity image of the welded metal surface has many noises. For this reason, we design a proper illumination system instead of usual illumination system such as halogen illumination. Through the experiment we know that the LED illumination source have a good result, and it is easy to handle, so that we use the LED illumination source.

In Fig. 4 (b) the camera is located at the vertical direction of the welded plate and the normal direction of the bead area is shown as N-direction. Two welded plates have different heights as shown in Figure. The LED illumination system is designed to have four directional illumination sources, positive and negative X Y-direction, each of them can turn on and off respectively. Each angle of four directions is properly designed to produce a uniform lighting condition at each welded surface. By using a- and c-side illumination source in Fig. 4(b) we can obviously observe the boundary of the bead, and using b- and d-side illumination source it help to investigate the bead pitch.

2.2 Two camera system

The narrow field of view camera can see the narrow area and the target in detail, so it is suitable for seeing the small object and making a close inspection of the target. In the contrary the wide field of view camera can see the wide area and the configuration of the target object, so it is suitable for investigating roughly the shape of target object. To use these facts in our study to detect the four defects effectively and fast with different field of view two cameras. The camera with narrow field of view($1.2\times0.9\ cm$) is used. It is used to detect bead shape abnormality, because the feature of these defects can be observed finely with the close locking camera. The another camera with wide field of view($3.05\times2.2\ cm$), and it is used to investigate the arc strike, scratch, and pitch abnormality, because we can well observe the configuration of these defects by using it. The designed system is shown in Fig. 5.

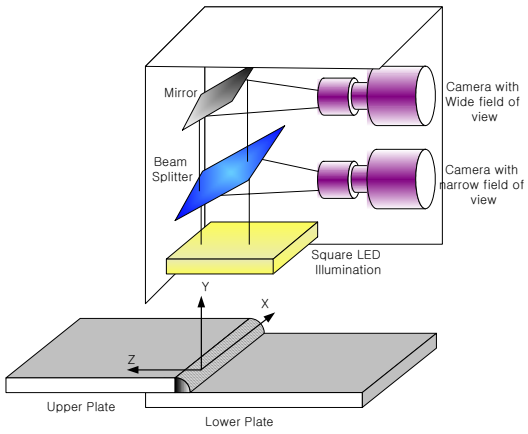

Fig 5. The schematic of two camera system

3. DEFECT DETECTION ALGORITHMS

Now we introduce an algorithm to detect defects. The defects have their own characteristics for shape feature and intensity, so we need to develop the algorithm properly for each defect. So we develop four different algorithms and introduce them in this chapter respectively.

The original image obtained from two cameras has many noise intensity values, though we using properly designed hardware systems, so we adapted the Gaussian Filtering to

reduce the noise. The Gaussian filtering is well known as the method to reduce the noise. After Gaussian filtering we can get the more quality raw image.

The detection algorithms must be brief, fast, and robust. The inspection area is very wide, so as considering the working effectiveness we must achieve the whole inspection process within 8 seconds for one step of the robot. Moreover the working environment is very harsh. Among the harsh environment to detect defects we make robust algorithms.

3.1 Algorithm to detect the bead shape abnormality

The bead shape abnormality is caused by improper welding operation and defects of the welding rod. The ordinary bead shape is almost rectangle, and the intensity value is lower than other plate surface in one obtained raw image with front illumination as shown in Fig. 6. The bead shape abnormality appeared simultaneously upper and lower boundary of the bead area. But we just investigate the lower boundary, because the bead shape abnormality is frequently detected at the lower boundary and it is difficult to discriminate the abnormality area for the upper bead boundary.

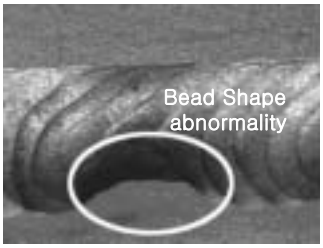

Fig 6. Intensity image of bead Shape abnormality

First we investigate the intensity deviation at each column. If the intensity deviation is bigger than the given threshold value, we assume that point as lower bead boundary. After finding the whole bead boundary point at each column we can easily make a lower boundary bead shape by fitting the line for selected points. By checking the distance between the fitted line and selected bead boundary, we can investigate the bead shape abnormality.

3.2 Algorithm to detect the bead pitch abnormality

The bead pitch abnormality is also caused by improper welding operation and defects of the welding rod. As shown in Fig. 7, we can see that the intersect part between two pitches have a lower intensity values than any other bead parts.

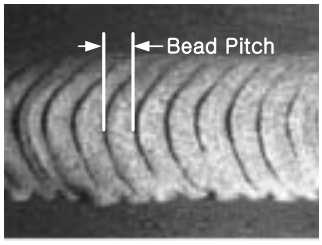

Fig 7. Intensity image of bead Pitch

Especially using the side illumination source, the intersection parts have been observed remarkably. In addition to that the bead part has a tendency which it is almost located at the horizontal direction of the middle in the raw image. Utilizing these tendencies, we can find the intersection parts between two neighbor pitches with image processing. Then if there is an abnormal distance value between estimated bead pitch, we assume that the bead pitch abnormality in the detected area.

3.3 Algorithm to detect the arc strike

The arc strike is appeared near the bead area and caused by splashing the welding arc. If the hot welding arc is sparking to the plate, it makes the small cone shape as shown in Fig. 8. The inner part of the cone shape has lower intensity value and outer part of one is looked brightly. That is to say that the intensity profile of the arc strike is U-type at the vertical and horizontal directions, and many arc strikes have similar shape profile. By experiment we know that the arc strike is obviously discriminated from other shapes at the edge feature image. In the edge feature image the arc strike is shown as the donut shape, which have inner and outer circle line. Using these tendencies we developed the algorithm to find an arc strike with image processing. In this process we can extract the bead area, because the arc strike rarely appeared at the bead part and though the arc strike is appeared at the bead area, it can detect as the bead pitch or bead shape abnormality.

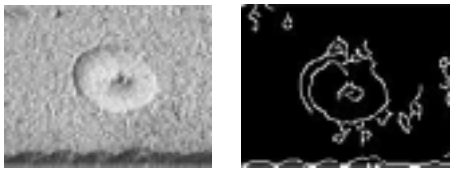

Fig 8. Intensity and edge image of arc strike

First we find candidate points, which have lower intensity value, have the U-type intensity profile horizontally and vertically, and have two circle lines in the edge image. Then for candidate points we estimate the normalized correlation coefficient with standard arc strike image as shown in Fig. 8. The equation of normalized correlation coefficient is as follows:

$$R(x,y)=\frac{\sum_{y'=0}^{h-1}\sum_{x'=0}^{w-1} I(x',y')I'(x+x',y+y')}{\sqrt{\sum_{y'=0}^{h-1}\sum_{x'=0}^{w-1} I(x',y')^2 \sum_{y'=0}^{h-1}\sum_{x'=0}^{w-1} I'(x+x',y+y')}}, \quad (1)$$

Where h and w is the height and width of the standard arc image, and I and I' is the intensity value of standard arc image and target image. If the normalized correlation coefficient has low value, the candidate point and area assume the arc strike point and area.

3.4 Algorithm to detect the scratch

The scratch is appeared near the surface of the bead area and caused by careless treatment of the plate steel. The feature of the scratch is also observed finely at the edge image. At the edge image the scratch is shown as two parallel white lines as shown in Fig. 9. In the intensity image the scratch area which is inside the parallel edge line has low intensity value. Using these tendencies we can find the scratch.

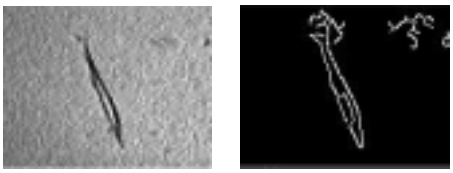

Fig 9. Intensity and edge image of scratch

First we find the candidate point which is between edge lines and the intensity value is low. Then we recursively find the next scratch candidate point which also has the characteristics which is same as the first candidate point among the 8-neighborhood pixels. If the number of candidate points is higher than the given threshold value, we regard these points and area as scratch.

4. EXPERIMENT AND RESULT

We verified the effectiveness of the inspection algorithm through the experiment with camera, zoom lens and LED illumination source. We can get the raw image from test equipment. Then we adapted the four developed algorithms. We captured the image for various cases; no defects, only one kind of defects, more two kinds of defects etc. For each case we tested developed algorithm and check the result. The effectiveness for each algorithm is checked by the task time and detection accuracy.

4.1 Bead shape abnormality

The bead shape abnormality is investigated by checking the distance between fitted line and selected boundary of the bead. We can verify the effectiveness of the algorithm by this experiment.

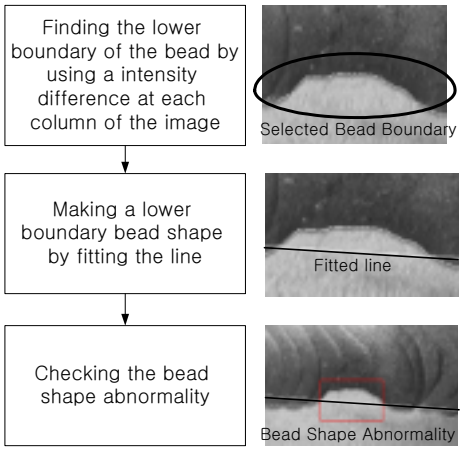

Fig 11. Bead shape abnormality

In Fig. 11, it shows that the bead shape abnormality is detected well. The task time is 1.534 seconds with Gaussian filtering. For other cases the bead shape abnormality is well detected. For the different experiments the algorithm runs well, and the detection accuracy is over 90% Through the experiments we can verify the effectiveness of the algorithm to detect the bead shape abnormality.

4.2 Bead pitch abnormality

The bead pitch abnormality is detected by checking the distance between the bead pitch. Unusual distances means that there is pitch abnormality. The algorithm is verified through the experiment with obtained images.

From Fig. 12 we can know that the pitch detection is performed well. The error between real pitch distance and estimated distance is less than 5% The task time is 1.438 second with Gaussian filtering. By this experiment we can verify the effectiveness of bead pitch abnormality.

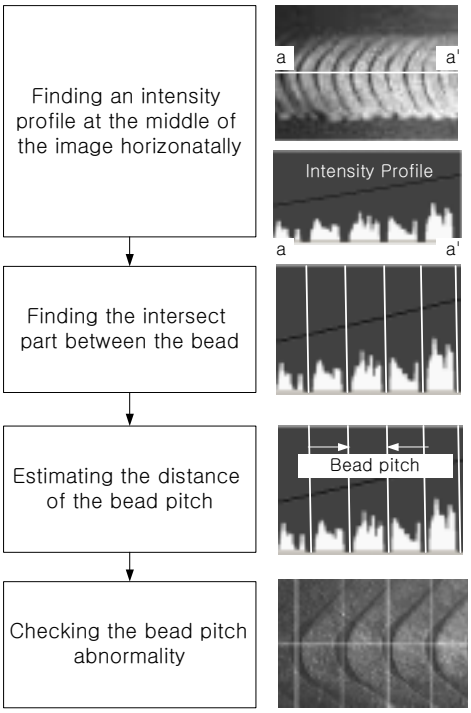

Fig 12. Bead pitch detection

4.3 Arc strike

The arc strike is detected with wide field view camera and side illumination source. The algorithm to detect the arc strike is verified by using these raw images and we can check a result as follows:

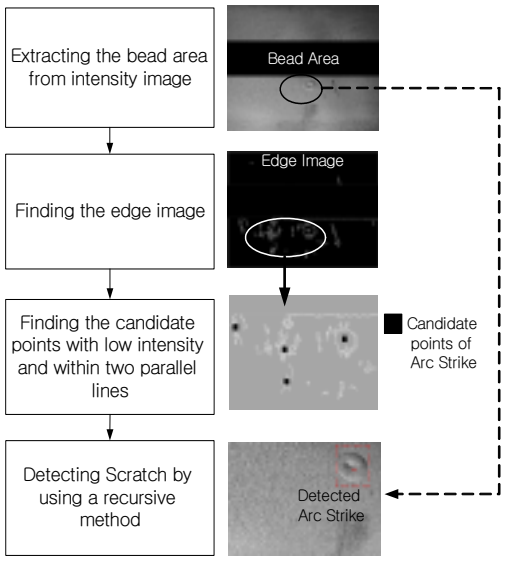

Fig 13. Intensity and edge image of arc strike

Fig. 13 shows that the result of the scratch and arc strike detection algorithm. The task time is 0.581.

The average task time with Gaussian filtering is 0.649 second for 20 test images, and just two times the algorithm failed. By these experiments we can verify the effectiveness of algorithm.

4.3 Scratch

The scratch is detected with wide field view camera and side illumination source. The algorithm to detect the scratch is verified by using these raw images and we can check a result as follows:

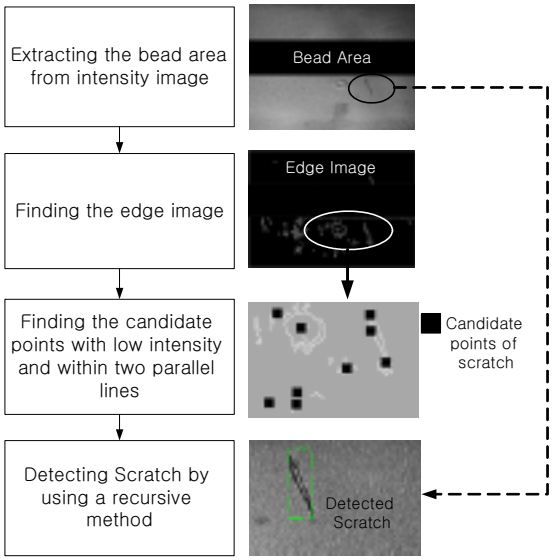

Fig 14. Intensity and edge image of arc strike

Fig. 14. shows that the result of the scratch detection algorithm. After adapting the detection algorithm we can successively find the scratch. The task time is 0.581. The average task time with Gaussian filtering is 0.649 second for 20 test images. By these experiments we can verify the effectiveness of algorithm.

5. CONCLUSION

First of all, to obtain the qualified raw image, we proposed the visual inspection system with the flexible LED illumination system and two camera system which has the different field of view. By using a common camera system and illuminations are limited to use in this harsh situation which the welded plate has high specular reflection and very many noises. To overcome them we design a new camera and illumination system. By using this system we can obtain the more qualified raw image.

Since the investigation environment is very harsh and the target task time is very short, the inspection algorithm for defects must be fast and robust. The proposed four algorithms to detect the defects satisfy these targets. The whole estimation time for performing the algorithms is 3.621seconds as a mean value. Though the obtained raw image still has very many noisy values, speckle and contamination noise, we can find the defects more than 90% accuracy. In addition, without classifier such as SOM etc. we successfully classified the defects using relatively simple four inspection algorithms based on just shape geometry. The experimental results shows the effectiveness of algorithms.

Table 2 Result of Algorithms

	Task time	Accuracy
Bead shape abnormality	1.534 sec	90%
Bead Pitch abnormality	1.438 sec	95%
Arc strike	0.649 sec	90%
Scratch		

ACKNOWLEDGMENTS

This study is the result from “The development of the inspection system of the welding defection” projects supported financially by Samsung Heavy Industry Co. Ltd.

REFERENCES

[1] Horikoshi, K., Shirakawa, Y., “An X-ray Radioscopy System for Pipe Weld Inspection Using a Real-time Image Integration Method,” *Transactions of the Society of Instrument and Control Engineers*, v.32 no.6, pp.811-819, 1996.

[2] Lantukh, V. M., “Acoustic inspection of austenitic butt welded joints in pipelines in electric power stations,” *Welding international*, v.10 no.9, pp.731, 1996.

[3] Lewis, P. A., Temple, J. A., Wickham, G. R., “Optimisation of ultrasonic inspection of welds in nuclear power plant,” *Insight : non-destructive testing and condition monitoring*, v.38 no.7, pp.496-501, 1996.

[4] Sethi, S. K., Ravi, B., Mohan, B. K., “Automated Visual Inspection of Cracks, in Cast and Welded Components,” *Transactions of the American Foundrymen's Society*, v.105, pp.819-824, 1998.

[5] Niskanen, M., Kauppinen, H., and Silven, O., “Real-time aspects of SOM-based visual surface inspection,” *Proceedings of SPIE--the international society for optical engineering*, no.4664, pp.123-134, 2002.

[6] Sosnin, F. R., “Visual Inspection of Welded Joints,” *Industrial laboratory*, v.64 no.2, pp.132-134, 1998.